Simulation of Rover Locomotion on Sandy Terrain - Modeling, Verification and Validation

Rainer Krenn, Gerd Hirzinger

German Aerospace Center, DLR, Institute of Robotics and Mechatronics
Oberpfaffenhofen, D-82234 Wessling, Germany
rainer.krenn@dlr.de, gerd.hirzinger@dlr.de

Abstract

In this paper a modeling technique called SCM (Soil Contact Model) for simulating the physical interaction between a rover mobility system (wheel, legs, tracks etc.) and a planetary soil surface will be presented. SCM computes the contact forces between the soil and the contact objects based on Bekker's empirical terramechanics formulae. Within SCM the soil geometry is described as digital elevation model (DEM) while the contact objects are described as general polygonal surface mesh grids. Based on this method SCM is able to deal with arbitrarily shaped contact objects without any restrictions in terms of application cases. Moreover, SCM provides a module for plastic soil deformation in order to take typical terramechanics phenomena like sinkage, bulldozing and multi-pass effects into account, which strongly affect the entire contact dynamics. The preferred simulation engine for SCM is SIMPACK, a 3D multi-body simulation package. In the verification process the correctness of the model has been demonstrated by bevameter tests proposed by Bekker. A first step in the validation process was made by applying SCM for simulations of ExoMars rover drawbar pull tests. It has been demonstrated that SCM creates simulation results with partly good correlation with real test measurements. Additional investigations are required for low contact velocities.

INTRODUCTION

In the recent years planetary exploration by means of mobile robotic systems became a more and more important issue within the space robotics community. Currently, ESA's ExoMars mission with its dedicated rover (Fig. 1) is one of the most powerful drivers in this field of research. But also smaller projects like the *Crawler* of DLR's Institute of Robotics and Mechatronics (Fig. 2) provide important contributions to the detailed understanding of rover locomotion on planetary terrains. A key science regarding rover locomotion is terramechanics. It addresses the interaction between wheels, legs or tracks of the rover and the soil surface in terms of sinkage and traction.

Fig. 1: Artist's View of ExoMars Rover

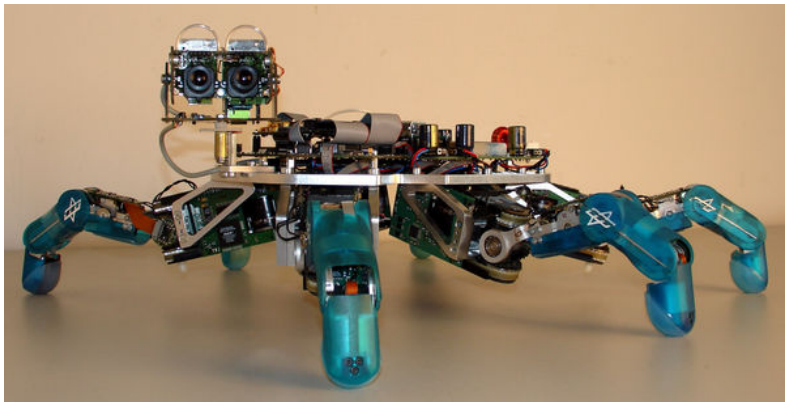

Fig. 2: DLR's Crawler

In the past a large number of various terramechanics based modeling and simulation approaches were presented. For the simulation of locomotion in sandy soil most of the authors apply the empirically found soil stress-strain laws as introduced by Bekker, e.g. [1] and extended by contributions of Wong [2]. An exemplary approach for the application of Bekker's theory is presented by Bauer, Barfoot et al. in [3]. Here, a tire-soil-interaction model has been validated versus experimental single-wheel tests such that the overall rover locomotion performance could be plausibly predicted. Ishigami, Yoshida et al. extended the single wheel setup to a full rover simulation with four steerable and controlled wheels in [4]. Herein, the complexity of the model was increased by taking bulldozing forces and lateral forces at the

wheels into account. The goal of our new approach was the extension of the current state of the art in wheel-soil interaction modeling such that the following requirements can be fulfilled:

1. Model compatibility with standard multi-body simulation engines like Matlab/Simulink and SIMPACK.
2. Applicability for arbitrary contact objects in order to be able to simulate the locomotion of systems others than wheeled ones like crawlers and trackers, and to be able to validate the model versus results of standard soil penetration tests like Bekker's bevameter experiments.
3. Computation of typical terramechanical phenomena like
    a. rolling resistance variations depending on sinkage (bulldozing),
    b. lateral constraint forces inside tracks depending on sinkage and lateral bulldozing,
    c. drawbar pull variations as function of slippage,
    d. multi-pass effects of wheels running inline in a track.

The according modeling activities resulted in a module called Soil Contact Model (SCM) that will be introduced in the following chapters. Moreover, a number of SCM performance tests will be presented, which have been accomplished for the verification and validation of the tool.

IMPLEMENTATION OF THE SOIL CONTACT MODEL (SCM)

The terramechanical contact problem soil – contact body can be generally described as the contact between a plastically deformable body and a rigid one. This implies that elastic deformations of the bodies, which penetrate the soil, are negligible in applications using SCM.

Soil Surface Description

The soil surface inside the SCM algorithm is described as a digital elevation grid DEM. It provides height information z at discrete horizontal coordinates x and y, which are defined by the grid nodes of a regular mesh grid. The distances between adjacent grid nodes are constant over the total surface. An example is given in Fig. 3. The contact counterpart is described as ordinary polygonal mesh grid with vertices and faces defining the body surface (Fig. 4).

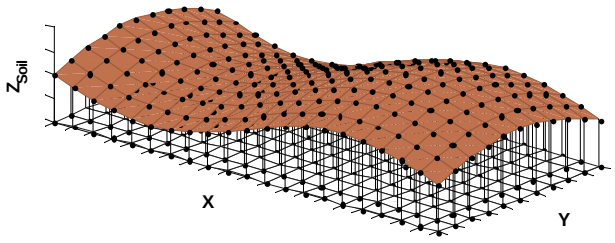

Fig. 3: Soil Surface Elevation Grid

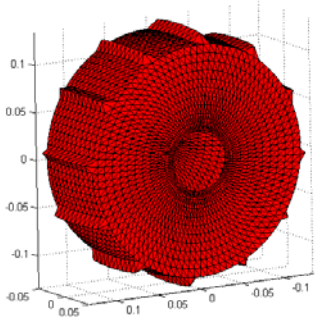

Fig. 4: Polygonal Surface of Contact Object (Wheel)

Beside the geometrical information each grid node of the soil is associated with a number of soil parameters and deformation states. The most important parameters of the soil grid nodes are collected in Tab. 1 together with two examples of planetary soil simulants.

Tab. 1: Soil Attributes of Grid Node

Parameters			Soil Simulant DLR-A	Soil Simulant DLR-D
Exponent of sinkage	n	[-]	0.63	1.8
Cohesive modulus	k_c	[N/m^{n+1}]	60300	-6.675e5
Frictional modulus	k_φ	[N/m^{n+2}]	2370	1.92e8
Cohesion	c	Pa	188	13
Internal friction	φ	deg	24.8	13.4

Contact Detection

For contact detection purposes the contact body is treated as a cloud of surface vertices (Fig. 5, a). In the second step the horizontal co-ordinates of the vertices will be mapped into the grid of the soil DEM such that the vertices will be arranged in columns afterwards (Fig. 5, b). Finally, the minimum vertices of each column (Fig. 5, c) will be selected for comparison with the vertical co-ordinates of the according soil grid nodes, respectively to detect contact and to define the footprint (Fig. 5, d). The footprint is the intersection volume of wheel and soil.

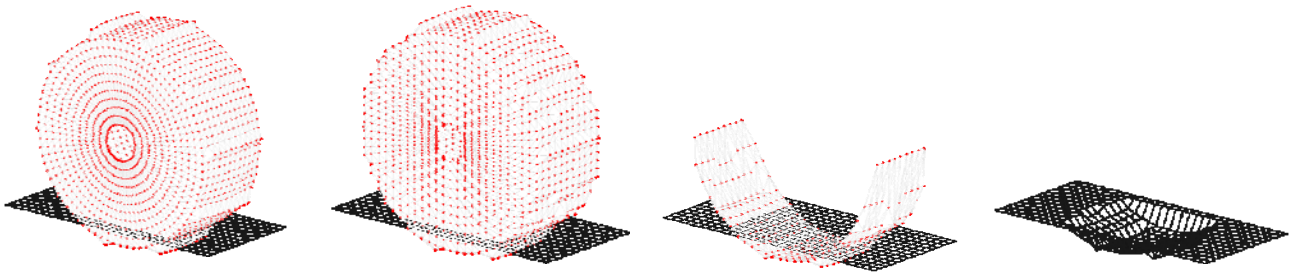

a) b) c) d)

Fig. 5: Contact Detection and Footprint Computation

Contact Force Computation

Once the contact is detected we are able to calculate the penetration depth z for each individual node of the footprint grid. Together with the soil parameters of Tab. 1 we have all pre-requisites for the computation of the local contact pressure p according to the empirical formula (1) of Bekker.

$$p = \left(\frac{k_c}{b} + k_\varphi \right) z^n \tag{1}$$

Herein, the variable b is representing a measure of the contact footprint shape. According to Bekker, b is the radius of a circular contact area or the length of the shorter side of a rectangular contact area. However, this definition is not applicable for a generally shaped footprint contour that changes during simulation. Therefore, SCM substitutes the variable b by b^*, which is a function of the total contact area size A and the total contact contour length U according to (2). Both, A and U can be easily tracked during simulation.

$$b^* = 2\frac{A}{U} \tag{2}$$

For circular contact planes b^* is identical with b and for rectangular contact planes b^* is a quite good approximation of b.

If the sinkage z is constant over the entire contact area A the pressure p according to (1) could be interpreted as the mean pressure acting in the contact zone. For the general case in SCM with individual sinkage of each grid node in the footprint the averaging approach is not valid anymore. Here, the pressure distribution inside the contact area has to be taken into account in order to provide correct results. In SCM the pressure distribution is derived from the centrality γ of contact grid nodes inside the contact area, which is a function of the distance to all other contact grid nodes (3).

$$\gamma = \frac{mR}{\sum_{i=1}^{m} R}; \quad R = \frac{1}{\sum_{j=1;j\neq i}^{m} \left(\left(\mathbf{r}_j - \mathbf{r}_i \right)^T \left(\mathbf{r}_j - \mathbf{r}_i \right) \right)}; \quad m = \text{number of contact grid nodes} \tag{3}$$

Examples for the centrality distribution are presented in Fig. 6. Taking the centrality (3) into account the original equation (1) has to be slightly adapted for use in SCM according to (4).

$$p^* = \gamma p = \gamma \left(\frac{k_c}{b} + k_\varphi \right) z^n \tag{4}$$

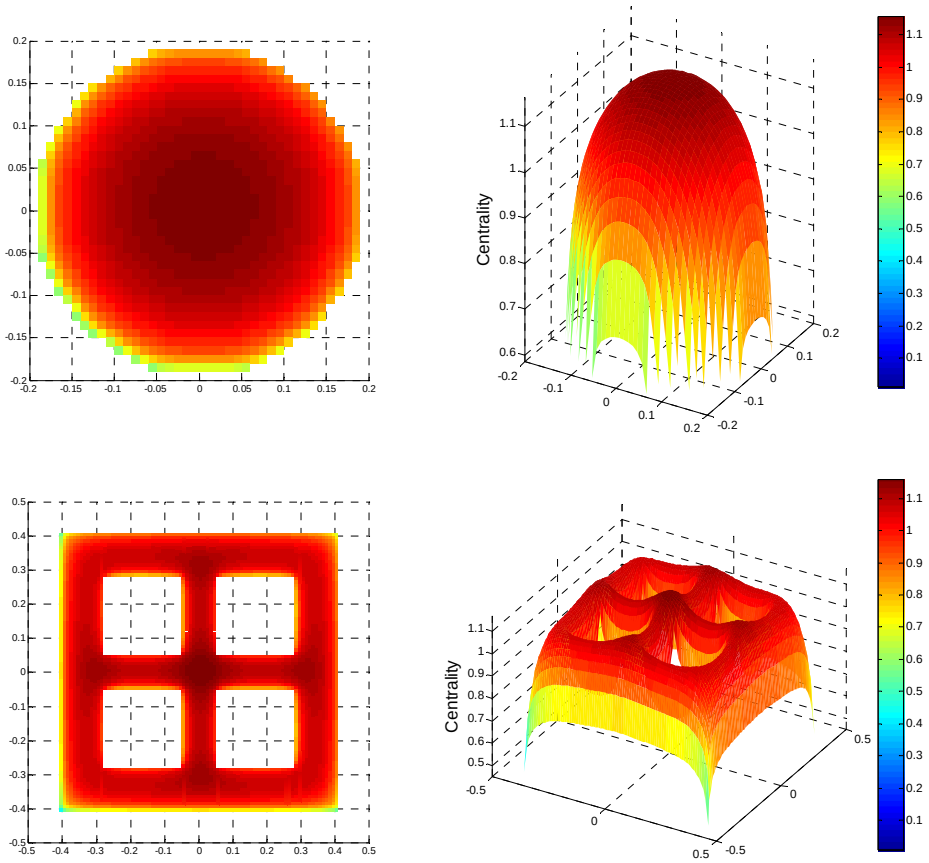

Fig. 6: Centrality Distribution over Contact Area Expressed by Color Mapping
Top: Circular contact area. Bottom: Grid like contact area)
Left: Vertical view on contact area. Right: Centrality distribution function

In order to be able to finally compute the contact forces, we have to take the soil surface normal vectors **n** and the relative velocity vectors **v** between soil surface and contact body surface into account. Based on them we can calculate normal soil penetration vectors **s** and tangential sliding vectors **t**. Assuming normalized vectors **s** and **t**, whose lengths are equal to the individual contact area sizes at the grid nodes, we can define the implemented components of the contact forces in SCM:

1. Sinkage resistance force:

$$\mathbf{F}_{Sinkage} = p^* \begin{pmatrix} 0 & 0 & 0 \\ 0 & 0 & 0 \\ 0 & 0 & 1 \end{pmatrix} \mathbf{s} \tag{5}$$

2. Bulldozing resistance force:

$$\mathbf{F}_{Bulldozing} = \left(c + p^* \tan\varphi\right) \begin{pmatrix} 1 & 0 & 0 \\ 0 & 1 & 0 \\ 0 & 0 & 0 \end{pmatrix} \mathbf{s} \tag{6}$$

3. Friction force as function of the friction coefficient μ between the soil and the contact body surface:

$$\mathbf{F}_{Friction} = \mu p^* \mathbf{t}; \quad \mu p^* < c + p^* \tan\varphi \tag{7}$$

Plastic Soil Deformation

The implementation of plastically deformable soils, respectively the footprint and landfill computation in SCM was motivated by typical rover simulation tasks. During cruising the front wheels are mostly rolling through untouched soil

with a significant bulldozing resistance that is typically increased by a hump in front of the wheel. On the other hand, the wheels following inline can drive in a pre-compressed rut at lower rolling resistance (multi-pass) but higher lateral guidance forces. The simulation of these phenomena requires a plastic deformation in the contact zone and an according deposition of the displaced soil. And the same requirements apply for simulating self-carving of wheels into soil under adverse conditions.

The algorithm for the plastic soil deformation, which is currently a first approach, is inspired by computer graphics algorithms for terrain generation (e.g. Olsen [5]) and animation of footprints in soil (e.g. Sumner et al. [6]). It consists of three steps:

1. Soil displacement from the contact area,
2. Temporary soil deposition at the border of the contact area and
3. Erosion of the displaced soil in the vicinity of the contact zone.

Soil Displacement

The total volume of the soil displacement is equal to the volume of the footprint that has been created by the contact body (Fig. 5, right). This implies that the total soil height reduction is equal to the wheel sinkage z at the according grid node. The displaced volume is divided into two parts dz who depend on the normal soil penetration vector $\mathbf{s}$. The parts are related to sinkage (7) and bulldozing motions (8).

$$dz_{sinkage} = z \cdot \frac{\mathbf{s}^T \begin{pmatrix} 0 & 0 & 0 \\ 0 & 0 & 0 \\ 0 & 0 & 1 \end{pmatrix} \mathbf{s}}{\mathbf{s}^T \mathbf{s}} \tag{8}$$

$$dz_{bulldozing} = z \cdot \frac{\mathbf{s}^T \begin{pmatrix} 1 & 0 & 0 \\ 0 & 1 & 0 \\ 0 & 0 & 0 \end{pmatrix} \mathbf{s}}{\mathbf{s}^T \mathbf{s}} \tag{9}$$

Temporary Soil Deposition

In this step the displaced soil volume will be temporary distributed over the border grid nodes of the footprint. So each border node gets a certain portion of each footprint node. The individual weighting factors w, which indicate how big the portions will actually be, depend on the distance vector $\mathbf{d}$ from the footprint node to the border node for sinkage (8) and the angle α between $\mathbf{d}$ and $\mathbf{s}$ for bulldozing (9).

$$w_{sinkage} = \frac{1}{\mathbf{d}^T \mathbf{d}} \tag{10}$$

$$w_{bulldizing} = \begin{cases} 0; & \cos\alpha \le 0 \\ \cos\alpha^m; & \cos\alpha > 0 \end{cases}; \quad \cos\alpha = \frac{\mathbf{d}^T}{|\mathbf{d}|} \frac{\mathbf{s}^T}{|\mathbf{s}|}; \quad m = 1,3,5\cdots \tag{11}$$

An impression for soil displacement and temporary deposition is given in Fig. 7. Here a wheel was rolling over the soil with a constant sinkage rate.

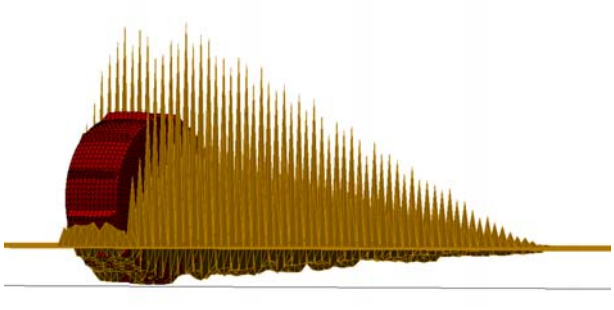

Fig. 7: Soil Shape Appearance After Displacement and Frozen, Temporary Deposition without Erosion

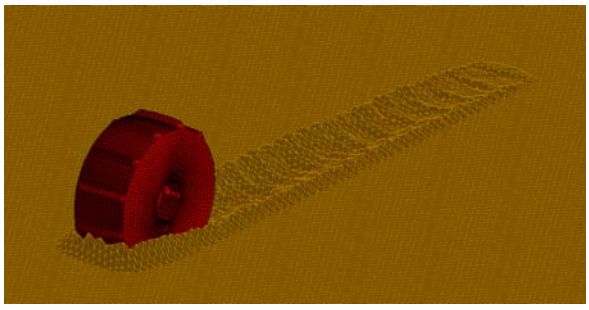

Fig. 8: Soil Shape Appearance After Soil Displacement, Deposition and Erosion

Erosion of Soil

When sand is piled a maximum sand hill slope angle can be achieved, which is equal to the internal friction angle φ of the sand. Therefore, after temporary deposition of the displaced soil volume SCM applies an erosion algorithm to the soil grid nodes in the vicinity of the contact area in order to meet this physical limitation. At soil grid resolution *ds* the maximum soil height difference dz_{Limit} to the adjacent nodes is limited as given in (12).

$$dz_{Limit} = ds \cdot \tan\varphi \tag{12}$$

In the erosion algorithm (13) half of the height that exceeds dz_{Limit} will be removed and added to the adjacent nodes according to their individual fraction of the total erosion potential.

$$dz_{erosion} = -\frac{\max(dz) - dz_{Limit}}{2} \cdot \frac{dz}{\sum_{i=1}^{4} dz_i}; \quad i = 1, \cdots, n \tag{13}$$

In Fig. 8 the result of the complete plastic soil deformation process is presented.

VERIFICATION

The verification process of SCM we have to prove, that the model generates correct results in terms of the implemented terramechanics, respectively Bekkers theory. In particular we have to prove that the computed contact forces, which are a function of the parameters of Tab. 1 and the relative kinematics between contact body and soil surface, match sufficiently the experimental results, where Bekkers theory is based on.

For the verification of SCM we apply the bevameter tests as proposed by Bekker. In this soil penetration tests probes of different sizes with circular or rectangular contact area will be pressed into the soil with a well defined vertical force. The according maximum penetration depth of the probe will be recorded. By varying probe size and penetration force we can identify the soil parameters of (1), k_c, k_φ and n, which describe the pressure – sinkage function.

Tab. 2 Verification of SCM – Parameter Identification

	n [-]	k_c [N/m^{n+1}]	k_φ [N/m^{n+2}]
	Applied Soil Parameters		
	0.63	2370	60300
Simulation Conditions	Identified Soil Parameters		
Resolution Soil/Probe = 0.005 m/0.005 m	0.6343	2271.48	62612.16
Resolution Soil/Probe = 0.0075 m/0.0075 m	0.6331	2357.78	63119.75
Resolution Soil/Probe = 0.01 m/0.01 m	0.6323	2351.08	61874.48

In Fig. 9 the results of the bevameter test simulations with cylindrical probes of two different diameters are presented. The verification references for all simulations are the ideal functions according to Bekker (1). In order to analyze the sensitivity of the simulation accuracy in terms surface shape discretization both, the soil grid resolution and contact body surface mesh grid resolution has been varied at each test (soil resolution >= contact body resolution). Generally we can state that SCM meets the ideal results very well and the impact of resolution variations is absolutely acceptable. This statement will be confirmed by the results of the soil parameter identification based the simulation results mentioned above. In Tab. 2 the identified soil parameters are presented. All of them match the originally applied parameters quite well.

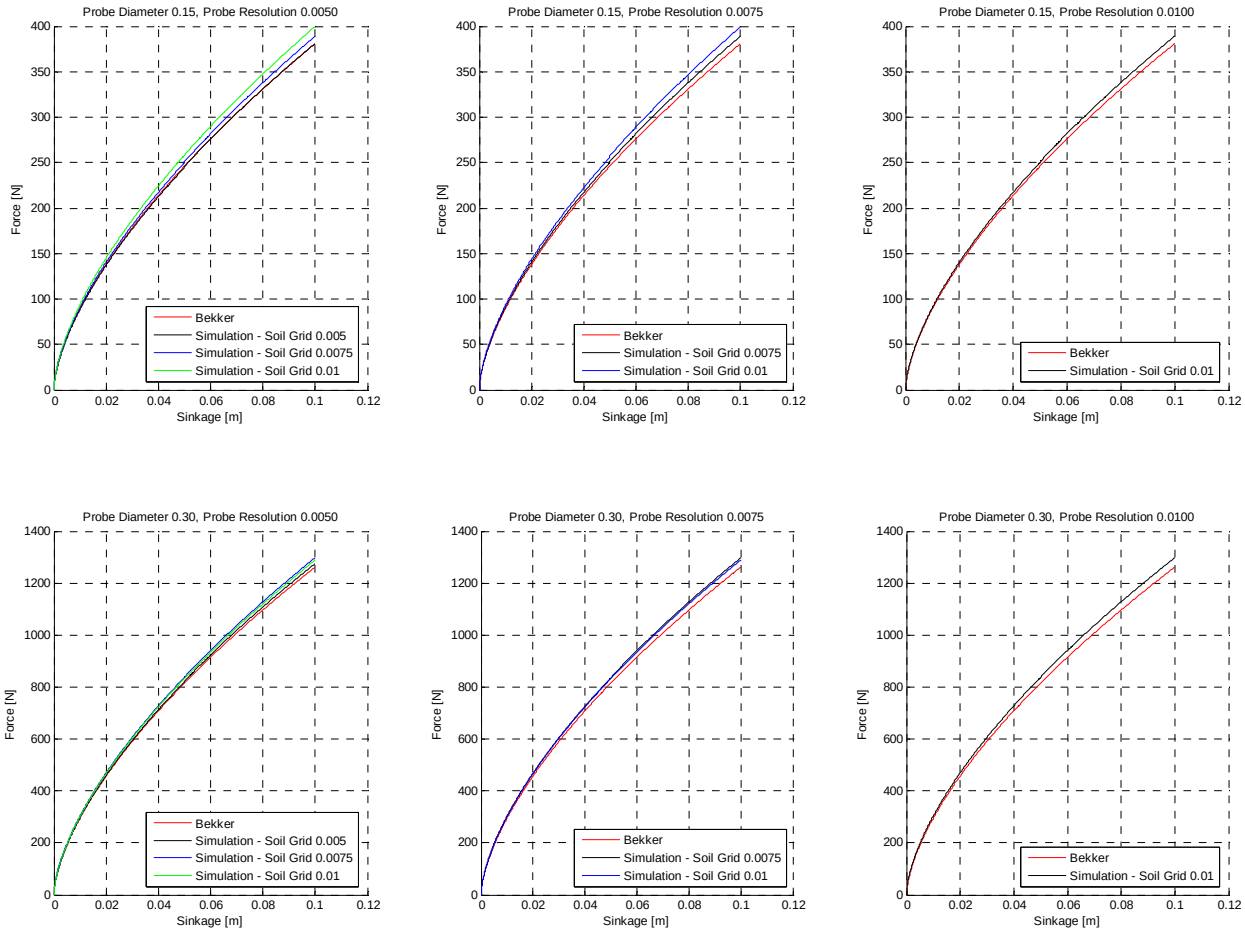

Fig. 9: Verification of SCM with Sensitivity Analysis (Mars Soil Simulant DLR-A, see Tab. 1)

VALIDATION

In the validation process we have to demonstrate, that SCM is able to simulate general terramechanical problems. This implies the question if the theory of Bekker is applicable without further problem specific adaptations. In the very first step of the SCM verification process the drawbar pull results of the ExoMars breadboard chassis test were taken as reference for according drawbar pull simulations with SCM. The tests were prepared and executed by ETH, Zurich at Oerlikon Space, Zurich. In Fig. 10 and Fig. 11 the scenario of the SCM simulation and the real breadboard chassis inside a soil stimulant testbed are presented.

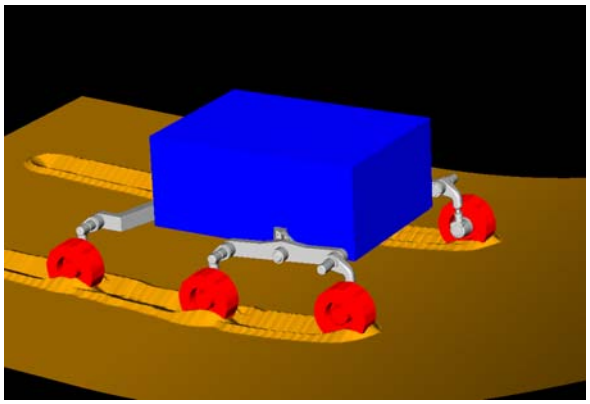

Fig. 10: Senario of Rover Simulations Using SCM and SIMPACK

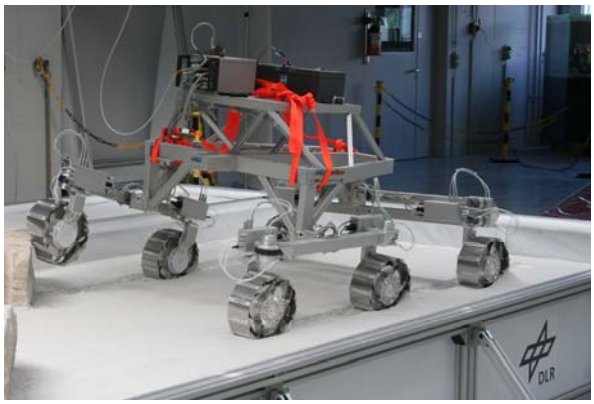

Fig. 11: ExoMars Breadboard Chassis, Oerlikon Space, Zurich

In the drawbar pull tests the rover chassis is tethered onto a wire that will be unrolled with controlled constant velocity v_{Tether}. The angular velocity of the rover wheels ω_{Wheel} is adjusted such that the desired rover velocity $v_{Rover,desired}$ would be slightly faster then the tether deploying velocity. But due to the velocity limitations of the tether, the wheels are well defined slipping in the sand. The relation between the slippage s and the velocities of tether and rover is the following:

$$s = 1 - \frac{v_{Tether}}{v_{Rover,desired}} = 1 - \frac{v_{Tether}}{\omega_{Wheel} r_{Wheel}}; \quad r_{Wheel} = \text{wheel radius}; \quad v_{Tether} = 0.0108 \ \frac{\text{m}}{\text{s}} \tag{14}$$

The applied pull force will be recorded by a sensor mounted between the rover and the tether. In Fig. 12 the drawbar pull forces of SCM simulations and the according measurements made during the ExoMars breadboard chassis tests are presented as function of slippage. In the diagram the force measurements, in particular the plots of drawbar pull force versus experiment time (e.g. small sub-diagram in Fig. 12), have been horizontally strongly compressed and placed close to the according slippage value in the diagram. By this method both, the function pull force versus slippage and the range of the force bandwidth of the forces can be presented in one diagram.

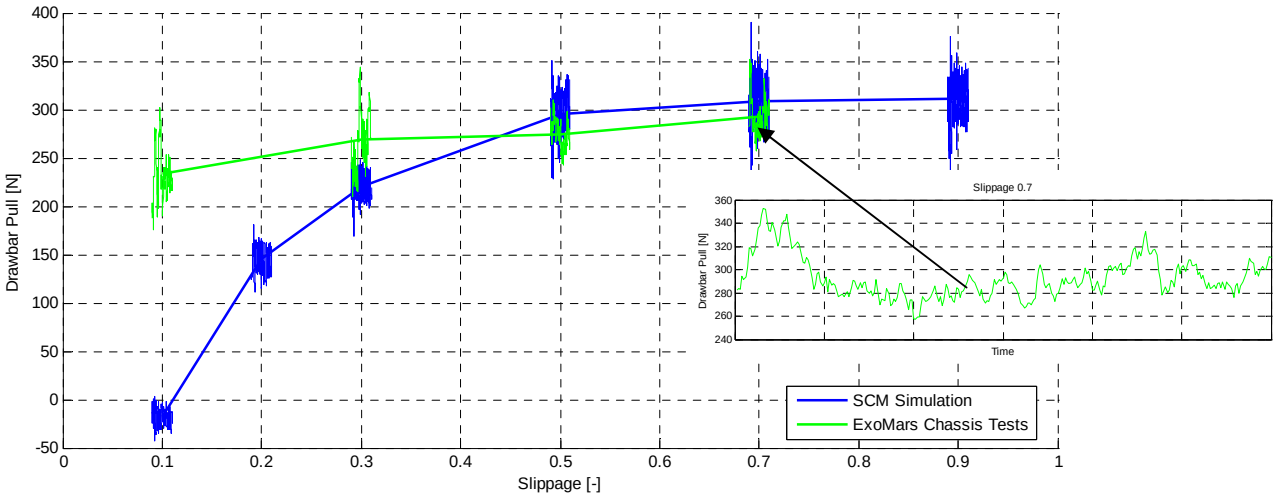

Fig. 12: Drawbar Pull as Function of Slippage (Mars Soil Simulant DLR-D, see Tab. 1)

The output of SCM simulations provides a “classical” function drawbar pull versus slippage with asymptotical approach to the maximum value. However, the real measurements came out with an atypical, almost linear function. Therefore, the simulation matches the real values only at slippage > 40%, respectively at higher relative velocities between wheels and soil, with sufficient accuracy. On the other hand, the bandwidth of the forces, which relates with the effects of the wheel grousers, can be reproduced by SCM quite well. Hence, the future focus of the SCM validation process will be the modeling of velocity dependent components of the soil contact dynamics.

REFERENCES

[1] M.G. Bekker, *Introduction to Terrain-Vehicle Systems,* The University of Michigan Press, Ann Arbor, USA, 1969

[2] J.Y. Wong. *Theory of Ground Vehicles*, Wiley, New York, 3rd Edition, 2001

[3] R. Bauer, W. Leung and T. Barfoot, *Experimental and Simulation Results of Wheel-Soil Interaction for Planetary Rovers,* IROS 2005, Edmonton, Alberta, Canada, 2-6 August 2005

[4] G. Ishigami, A. Miwa, K. Nagatani and K. Yoshida, *Terramechanics-Based Model for Steering Maneuver of Planetary Exploration Rovers on Loose Soil,* Journal of Field Robotics 24(3), pp 233-250, Wiley InterScience, 2007

[5] J. Olsen, *Realtime Procedural Terrain Generation,* IMADA, University of Southern Denmark, 31 October, 2004

[6] R.W. Sumner, J.F. O´Brien and J.K. Hodgins, *Animation Sand, Mud and Snow,* Computer Graphics Forum, Volume 18, No 1, 1999